Advances in Science and Technology Research Journal

Advances in Science and Technology Research Journal, 2027, 21(1), 44–64
https://doi.org/10.12913/22998624/22687
ISSN 2299-8624, License CC-BY 4.0

Received: 2026.07.17
Accepted: 2026.11.15
Published: 2026.12.01

Heat-treatment-induced hardness–toughness trade-off, anisotropy reduction and fracture-mode transition in direct metal laser sintering Ti6Al4V

Żaneta Anna Mierzejewska[1*], Anna Falkowska[2], Stanisław Dzielak[1]

[1] Institute of Biomedical Engineering, Faculty of Mechanical Engineering, Bialystok University of Technology, Wiejska 45C, 15-351 Bialystok, Poland
[2] Department of Mechanics and Applied Computer Science, Faculty of Mechanical Engineering, Bialystok University of Technology, Wiejska 45C, 15-351 Bialystok, Poland; a.falkowska@pb.edu.pl
* Corresponding author's e-mail: a.mierzejewska@pb.edu.pl

ABSTRACT

Direct metal laser sintering (DMLS), considered here as a process-specific implementation of laser powder bed fusion (LPBF), produces Ti6Al4V with a fine acicular α′-type morphology, high hardness, residual stresses, and orientation-dependent mechanical behaviour. This study quantified the effect of annealing temperature on the coupled evolution of microhardness, Charpy impact toughness, mechanical anisotropy, and fracture morphology. Ti6Al4V ELI specimens were fabricated in XY and XZ orientations at a volumetric energy density of 127 J/mm³ and annealed at 650, 750, 850, or 950 °C for 2 h under argon. Mechanical response was evaluated by HV5 measurements (at least nine indentations per measurement plane), Charpy testing (n = 3 per heat-treatment condition and orientation), and SEM-based microstructural and fractographic assessments. At 950 °C, perpendicular-plane hardness decreased by 18.8% (401.7 ± 20.8 to 326.0 ± 5.6 HV5), whereas mean impact toughness increased by 266.8% (14.29 ± 2.50 to 52.41 ± 8.50 J/cm²). The hardness anisotropy coefficient decreased by 5.8%, from 1.078 to 1.015, and the impact-toughness anisotropy coefficient decreased by 26.2%, from 1.397 to 1.031. SEM observations showed a progressive transition from defect-sensitive quasi-brittle fracture toward predominantly ductile microvoid coalescence. Annealing at 850–950 °C, therefore, produced the most favourable balance between retained hardness, enhanced impact resistance, reduced orientation dependence and ductile fracture behaviour.

Keywords: Ti6Al4V, DMLS, LPBF, heat treatment, microhardness, Charpy impact toughness, anisotropy, fractography.

INTRODUCTION

Additive manufacturing technologies have transformed modern materials engineering by enabling the production of geometrically complex components with reduced material waste and substantial design flexibility [1,2]. Among metal additive manufacturing methods, direct metal laser sintering (DMLS), here treated as a commercial/process-specific implementation of the broader LPBF technology group, is widely used for processing titanium alloys [3,4]. Ti6Al4V is particularly attractive for aerospace, biomedical, and energy-related applications because it combines high specific strength, corrosion resistance, low density and favourable biocompatibility [5,6].

Despite these advantages, the mechanical behaviour of DMLS/LPBF-produced Ti6Al4V differs significantly from conventionally manufactured material. During LPBF, powder particles are subjected to very high heating and cooling rates, which suppress equilibrium transformations and promote the formation of a metastable acicular α′ martensitic morphology. The resulting material is characterised by

high hardness and strength, but also by residual stresses and orientation-dependent mechanical behaviour related to elongated prior-β grains, melt-pool geometry, and repeated layer-wise thermal cycling [7,8].

Mechanical anisotropy remains a major qualification challenge for additively manufactured titanium alloys. Murthy et al. [6] demonstrated orientation-dependent room-temperature strength and ductility in LPBF Ti6Al4V-ELI and linked the response to directional prior-β grains and texture. Cao et al. [4] further showed that build orientation, melt-pool architecture, and defect morphology jointly affect tensile, fatigue, and fracture behaviour. More recent work has confirmed that thermal treatment reduces the mechanical significance of the original directional microstructure by promoting α′ decomposition, stress relaxation and α + β stabilisation [9–11]. These studies established the importance of anisotropy, but they generally emphasise tensile properties, phase evolution or a single post-processing condition rather than the coupled temperature-dependent evolution of hardness, impact toughness and fracture mode.

Dynamic fracture behaviour remains less frequently quantified than tensile performance. Zhang et al. [7] reported improved Charpy response after sub-transus heat treatment of LPBF Ti6Al4V, while Monaheng et al. [12] demonstrated that a two-stage thermal cycle can increase the impact resistance of LPBF Ti6Al4V-ELI. Fractographic studies of additively manufactured metals show that pores, lack-of-fusion discontinuities, and unmelted particles act as preferential crack-initiation sites, whereas increased microvoid coalescence reflects greater plastic energy dissipation. Macek et al. [10], although investigating additively manufactured AISI H13 steel, rather than titanium, provided a detailed framework linking AM-induced porosity, local fracture morphology, and crack-propagation mechanisms; this framework is directly relevant to the interpretation of the present SEM observations.

Post-processing heat treatment is used to relax residual stresses and transform the metastable α′-type morphology toward a more stable α + β condition. Vrancken et al. [13] established a strong dependence of the Ti6Al4V mechanical properties on annealing temperature and cooling route. Etesami et al. [14] subsequently synthesised the correlations among thermal cycle, phase morphology and mechanical response. Boccardo et al. [9] showed in situ that β nucleates mainly along α′-lath boundaries during decomposition and that visible morphological coarsening becomes pronounced above approximately 700 °C. Recent studies from 2024–2026 have likewise reported stabilisation and coarsening of α + β lamellae, reduced hardness gradients and reduced orientation sensitivity after sub-transus treatment [11,15,16].

The current literature therefore identifies three partially separated research streams: optimisation of tensile properties, characterisation of microstructural transformation, and assessment of build-orientation effects. The fundamental difference of the present study is that it integrates four annealing temperatures (650–950 °C), two build orientations, two complementary mechanical metrics with opposing trends, quantitative anisotropy coefficients, and SEM fracture-mode assessment within one experimental framework. This design makes it possible to identify not merely whether heat treatment is beneficial, but how the hardness–toughness compromise and orientation dependence evolve across the sub-transus temperature range.

Understanding the relationship between thermal exposure, mechanical anisotropy and fracture behaviour is particularly important for engineering applications requiring a balance between hardness and damage tolerance. Excessively hard martensitic structures may provide high resistance to plastic deformation but often exhibit reduced ability to dissipate fracture energy. Conversely, microstructural softening induced by heat treatment may improve toughness at the expense of hardness. Identifying an optimal compromise between these properties remains essential for the reliable design of DMLS Ti6Al4V components. From an engineering design perspective, experimentally determined mechanical characteristics of DMLS Ti6Al4V are also important as input and validation data for numerical simulations. Reliable finite element analyses, damage models, and computer-aided optimisation procedures require the material parameters that reflect the actual effects of build orientation, heat treatment and fracture mechanisms. Such datasets may support predictive assessment of mechanical performance without the need to manufacture and destructively test numerous additional specimens for each processing condition. Therefore, linking experimental characterisation with future numerical modelling provides a practical

route for reducing trial-and-error testing while improving the reliability of additively manufactured titanium components.

Therefore, the aim of the present study was to investigate the influence of post-processing heat treatment on the microhardness, Charpy impact toughness, anisotropy and fracture mechanisms of DMLS-produced Ti6Al4V alloy. The specimens fabricated under optimized processing conditions were subjected to annealing at temperatures ranging from 650 °C to 950 °C. Mechanical characterisation was performed using Vickers microhardness and Charpy impact testing, while fracture surfaces were analysed by scanning electron microscopy. Particular attention was devoted to the evolution of the hardness–toughness relationship and to the reduction of anisotropic behaviour associated with thermally induced microstructural transformations.

The novelty of the work lies in the simultaneous quantification of: (i) the temperature-dependent hardness–toughness trade-off; (ii) hardness and Charpy anisotropy in two build orientations; and (iii) the accompanying transition from defect-sensitive quasi-brittle fracture to ductile microvoid coalescence. Unlike studies limited to a single thermal condition or tensile endpoints, the present four-temperature series allows identification of the 850–950 °C range as the interval in which toughness gains and anisotropy reduction become pronounced while useful hardness is retained.

MATERIALS AND METHODS

Material and DMLS fabrication

The investigated material was Ti6Al4V alloy powder (Grade 23, ELI) processed using DMLS. The powder was manufactured by gas atomisation and supplied for biomedical-grade LPBF applications. The particles exhibited predominantly spherical morphology with a nominal particle-size range of 15–45 µm. The material complied with the Ti6Al4V ELI composition range, with Ti as the balance as well as Al and V as the principal alloying elements.

All specimens were fabricated using an EOSINT M280 system (EOS GmbH, Germany) equipped with a Yb-fiber laser operating under a protective argon atmosphere. During fabrication, the oxygen concentration inside the build chamber was maintained below 0.13% to minimise oxidation and contamination of the titanium alloy. DMLS was used throughout the manuscript as the machine/process-specific term, whereas was is used when discussing the broader additive-manufacturing literature.

Based on previous optimisation studies focused on porosity reduction and mechanical performance [17,18], a volumetric energy density of 127 J/mm³ was selected for specimen fabrication. This processing condition provided the lowest porosity level and the most homogeneous microstructure among the investigated manufacturing parameters. The volumetric energy density was calculated according to Equation 1:

$$E_s = P / (v \cdot h \cdot t) \quad (1)$$

where: E_s is the volumetric energy density (J/mm³), P is the laser power (W), v is the scanning speed (mm/s), h is the hatch spacing (mm), and t is the layer thickness (mm). The principal DMLS processing parameters are summarised in Table 1.

To evaluate the influence of manufacturing anisotropy, specimens were fabricated in two build orientations. In the horizontal orientation (XY), the longitudinal axis of the specimen was parallel to the build platform. In the vertical orientation (XZ), the specimen axis was aligned with the build direction. Following fabrication, support structures were removed by electrical discharge machining, and the specimens were lightly ground to remove residual surface irregularities (Figure 1).

Table 1. DMLS processing parameters and post-processing heat treatment conditions

Parameter	Value
Laser power	190 W
Scanning speed	500 mm/s
Layer thickness	0.03 mm
Hatch spacing	0.10 mm
Laser beam diameter	0.10 mm
Build platform temperature	200 °C
Protective atmosphere	Argon
Volumetric energy density	127 J/mm³
Build orientations	XY, XZ
Heat treatment temperatures	650, 750, 850, 950 °C
Holding time	2 h
Cooling schedule	Furnace cooling to 500 °C + air cooling

Heat treatment procedure

Post-processing heat treatment was performed in a vertical tube furnace under continuous high-purity argon. The temperatures were selected a priori from the Ti6Al4V transformation literature and from the authors' previous DMLS optimisation work [9, 13, 14, 17, 19]. Specifically, 650 °C represents a stress-relief/decomposition-onset condition; 750 °C captures the transitional interval in which visible α′-morphology modification becomes more evident; 850 °C represents advanced sub-transus α + β development and corresponds to the authors' earlier favourable condition; and 950 °C approaches the β-transus while remaining sub-transus, enabling substantial lamellar coarsening without full β-field treatment. The 100 °C increments were chosen to provide a systematic comparison across these metallurgically distinct regimes rather than to optimise a single proprietary cycle. For each condition, specimens were held for 2 h. The heating rate was approximately 10 °C/min. The furnace was then cooled to approximately 500 °C under argon at an average rate of 2.4 °C/min (approximately 0.04 °C/s), followed by air cooling to room temperature. The as-built state served as the reference condition.

Charpy impact toughness testing

Impact toughness was determined using the Charpy method according to PN-EN ISO 148-1. V-notched specimens were machined from DMLS-fabricated material using wire electrical discharge machining to minimise thermal distortion and residual machining stresses. The absorbed fracture energy was normalised to the cross-sectional area at the notch root, allowing the results to be expressed as impact toughness values in J/cm².

Testing was performed at room temperature using an instrumented pendulum impact tester. The absorbed fracture energy was recorded for each specimen and converted into impact toughness values according to Equation 2:

$$K_c = K / A \tag{2}$$

where: K_c is the impact toughness (J/cm²),
K is the absorbed fracture energy (J),
and A is the cross-sectional area at the notch root (cm²).

A minimum of three specimens was tested for each heat-treatment condition and, where build orientation was evaluated, for each orientation separately. Results are presented as mean values with corresponding standard deviations. The small number of Charpy specimens should be considered when interpreting differences between

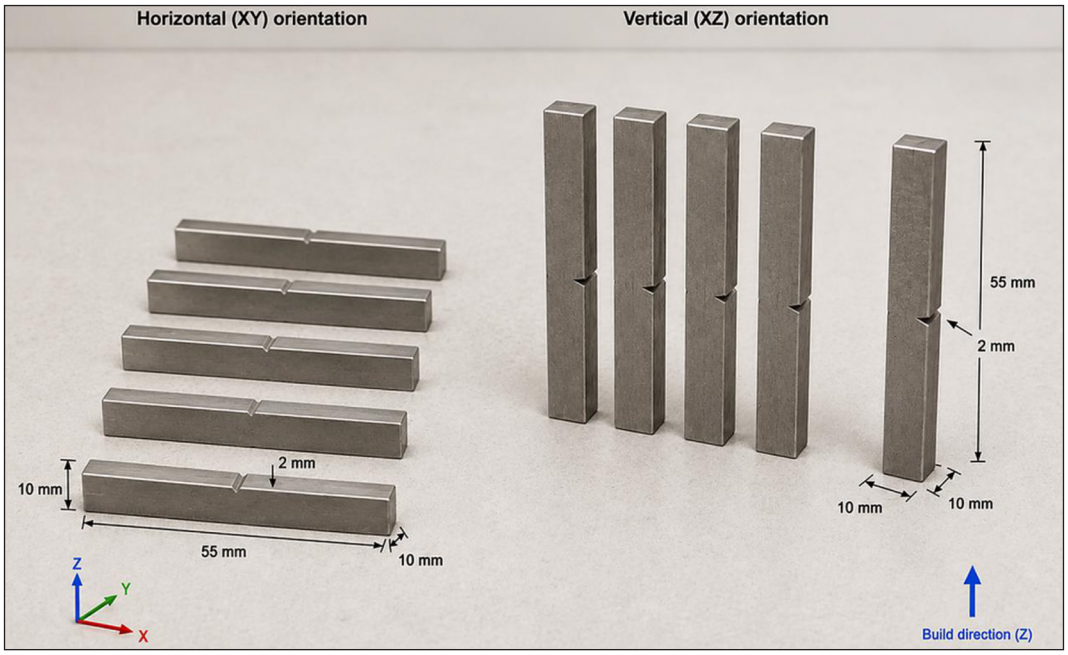


Figure 1. Schematic of the two specimen build orientations used in this study relative to the DMLS build direction: the horizontal (XY) orientation, with the specimen longitudinal axis parallel to the build platform, and the vertical (XZ) orientation, with the specimen axis aligned with the build direction

adjacent annealing temperatures, particularly between 850 and 950 °C.

Both horizontal (XY) and vertical (XZ) specimens were examined in the as-built state and after heat treatment. In the horizontal orientation (XY), the longitudinal axis of the specimen was parallel to the build platform, whereas in the vertical orientation (XZ), the longitudinal axis was aligned with the build direction. The symbols ⊥ and ∥ refer to loading/fracture configurations evaluated relative to the deposited layers; this notation was used consistently for the calculation of anisotropy coefficients.

Microhardness measurements

Microhardness measurements were performed using the Vickers method in accordance with PN-EN ISO 6507-1. A diamond pyramidal indenter and a test load of 5 kgf (HV5) were applied.

Measurements were conducted on polished metallographic cross-sections prepared from both horizontally and vertically fabricated specimens. To evaluate the directional effects associated with the layer-by-layer manufacturing process, hardness was measured on two characteristic planes:

- perpendicular to the deposited layers (⊥),
- parallel to the deposited layers (∥).

At least nine indentations were performed on each measurement plane. The spacing between adjacent indentations was selected to avoid interaction between neighbouring plastic zones. Mean hardness values and standard deviations were subsequently calculated for each condition.

The influence of heat treatment temperature on hardness evolution was analysed and correlated with impact toughness and fracture morphology.

Metallographic preparation and fractographic analysis

Microstructural characterisation and fracture surface observations were carried out using scanning electron microscopy (SEM).

The specimens intended for metallographic examination were sectioned, mounted in conductive resin, and successively ground using SiC abrasive papers up to 2000 grit. Final polishing was performed using colloidal silica suspension. The polished surfaces were etched using Kroll's reagent, consisting of 92 mL distilled water, 6 mL nitric acid (HNO3), and 2 mL hydrofluoric acid (HF) for approximately 10–20 s, followed by rinsing in distilled water and ethanol drying.

For semi-quantitative microstructural assessment, α-lath or α-lamella width was estimated from representative SEM micrographs using the embedded scale bars and was cross-checked against literature values reported for heat-treated LPBF/DMLS Ti6Al4V.

Fractographic investigations were conducted on fractured Charpy specimens. After testing, fracture surfaces were cleaned in ethanol using an ultrasonic bath and dried in compressed air. SEM observations were performed using a Hitachi S-3000N scanning electron microscope (Hitachi High-Technologies, Tokyo, Japan) operated in secondary electron mode at an accelerating voltage of 15 kV.

Special attention was devoted to cleavage-like facets, microvoid coalescence, ductile tearing, crack-initiation sites, pores, lack-of-fusion regions, and unmelted particles. Fracture morphology was additionally classified semi-quantitatively using three predefined regimes: quasi-brittle, mixed, and predominantly ductile. Classification was based on the relative visual predominance and spatial continuity of cleavage-like/flat regions versus dimpled microvoid-coalescence regions across representative fields acquired under comparable SEM conditions. Because the archived images did not provide a sufficiently large, systematically randomised field set for unbiased stereological area-fraction or dimple-size statistics, numerical percentages were not reported; this restriction is stated explicitly to avoid over-interpretation of selected micrographs.

Porosity and lack-of-fusion defects were evaluated qualitatively from SEM observations of metallographic sections and fracture surfaces. Quantitative porosity assessment by micro-CT or systematic image analysis was not performed in the present dataset and is therefore reported as a limitation, rather than as a controlled variable.

Statistical analysis

The experimental results were presented as mean values ± standard deviation. Statistical analysis was performed using one-way analysis of variance (ANOVA) followed by Tukey's post hoc test for multiple comparisons. Heat-treatment conditions were compared separately for HV5⊥, HV5∥ and mean Charpy impact toughness. Differences were considered statistically significant

at $p < 0.05$. For microhardness, the interpretation was based on condition-level hardness trends and the measurement-plane effect rather than on individual indentation positions alone. Additionally, Pearson correlation analysis and linear regression were used to evaluate the relationship between microhardness and impact toughness. Because the correlation was calculated from group mean values, it is interpreted as a structure–property trend rather than a predictive model. Due to the limited number of Charpy specimens per condition, differences between adjacent heat-treatment groups were interpreted cautiously, particularly for the 850 and 950 °C conditions.

RESULTS

Microstructural evolution during heat treatment

Representative microstructures of DMLS-produced Ti6Al4V alloy in the as-built and heat-treated conditions are presented in Figure 2. The SEM observations revealed progressive morphological changes with increasing annealing temperature. Because X-ray diffraction and EBSD were not performed in the present dataset, the phase-related interpretation is based on SEM morphology and established transformation behaviour reported for heat-treated LPBF/DMLS Ti6Al4V. Therefore, the observed changes should be interpreted as morphological features consistent with α′ martensite decomposition, rather than direct crystallographic phase confirmation [7,13,19–21].

The as-built specimens exhibited a characteristic fine acicular martensitic morphology contained within elongated prior β grains oriented along the build direction (Figure 2a). The microstructure consisted of fine needle-like laths produced by extremely high cooling rates inherent to the DMLS process. This morphology is commonly associated with elevated hardness, high residual stresses, and pronounced anisotropic mechanical behaviour.

Following heat treatment at 650 °C for 2 h (Figure 2b), the overall morphology remained similar to that observed in the as-built condition. Acicular features were still clearly visible, although slight coarsening of individual laths could be observed. At this temperature, stress relaxation appears to be the dominant metallurgical process, while microstructural transformation remains limited.

More pronounced changes occurred after annealing at 750 °C (Figure 2c). The acicular morphology became less distinct, and SEM features consistent with the onset of α′ decomposition were observed. Fine lamellae separated by thin interlamellar regions began to develop within the prior martensitic structure. This transitional morphology corresponds to the temperature range where substantial changes in mechanical behaviour were first detected.

Heat treatment at 850 °C (Figure 2d) resulted in significant modification of the microstructure. The original martensitic morphology was largely replaced by a developed lamellar α + β-type morphology. The reduction of acicular features indicates advanced thermally induced microstructural rearrangement. This microstructural state coincided with a marked increase in impact toughness and a substantial reduction in hardness anisotropy.

The most extensive morphological modification was observed after annealing at 950 °C (Figure 2e). The microstructure consisted predominantly of coarse lamellar colonies with only limited remnants of the original acicular morphology. The increased lamellar thickness and greater microstructural homogeneity indicate advanced stabilisation of the alloy. This condition corresponded to the lowest hardness and highest impact toughness values measured in the present study.

Table 2. Semi-quantitative α-lath/α-lamella width estimated from representative SEM micrographs

Condition	α-lath / α-lamella width [μm]	Interpretation
As-built	0.59 ± 0.26	Fine acicular α′-type lath morphology
650 °C / 2 h	0.70 ± 0.22	Slight lath coarsening; stress-relief-dominated state
750 °C / 2 h	0.95 ± 0.25	Transitional acicular/early lamellar morphology
850 °C / 2 h	1.55 ± 0.22	Developed lamellar morphology; advanced α′ decomposition features
950 °C / 2 h	2.30 ± 0.40	Coarse lamellar morphology; high-temperature sub-transus coarsening

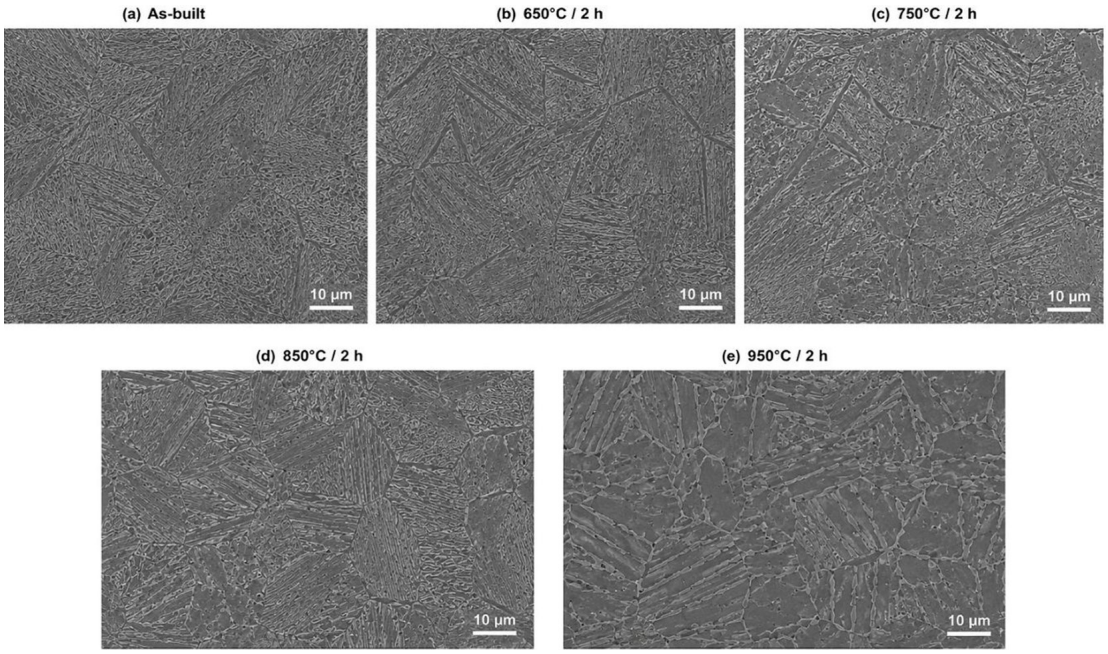


Figure 2. SEM micrographs showing the microstructural evolution of DMLS Ti6Al4V as a function of post-processing annealing temperature: (a) as-built condition – fine acicular α′ martensitic laths confined within elongated prior-β grains aligned with the build direction; (b) 650 °C/2 h – retained acicular morphology with slight lath coarsening, consistent with a predominantly stress-relief state; (c) 750 °C/2 h – transitional morphology in which acicular features become less distinct and early lamellar separation appears, indicating the onset of α′ decomposition; (d) 850 °C/2 h – developed lamellar α + β-type morphology with substantially reduced acicular character; (e) 950 °C/2 h – coarse lamellar colonies with only minor remnants of the original acicular structure, reflecting advanced sub-transus coarsening and microstructural homogenisation. Specimens etched with Kroll's reagent. Microstructural observations were performed on representative metallographic sections from each condition; HV5 testing comprised at least nine indentations per measurement plane

The observed microstructural evolution indicates that increasing annealing temperature progressively changes the highly strained acicular morphology generated during DMLS processing toward a more thermally stabilised lamellar α + β-type morphology. This transformation is accompanied by relaxation of residual stresses and reduction of directional microstructural features, providing a plausible explanation for the subsequent changes in hardness, impact toughness and fracture behaviour. Semi-quantitative SEM assessment supported the qualitative observation of progressive lamellar coarsening with increasing annealing temperature. The estimated α-lath/α-lamella width increased from approximately 0.59 µm in the as-built condition to approximately 2.30 µm after annealing at 950 °C (Table 2), consistent with reported coarsening of α/α′ laths during sub-transus heat treatment of LPBF/DMLS Ti6Al4V [1,7,19,21,22].

Evolution of microhardness and anisotropy after heat treatment

The microhardness results obtained for DMLS-produced Ti6Al4V alloy in the as-built and heat-treated conditions are presented in Table 3. Under all investigated conditions, the hardness measured on planes perpendicular to the deposited layers (⊥) was higher than that measured parallel to the deposited layers (∥), confirming the anisotropic character of the additively manufactured microstructure.

The highest hardness values were recorded in the as-built condition, reaching 401.7 ± 20.8 HV5 on the plane perpendicular to the deposited layers and 372.7 ± 13.4 HV5 on the parallel plane. These elevated hardness values are characteristic of the rapidly solidified martensitic α′ microstructure formed during the DMLS process. The extremely high cooling rates associated with laser powder bed fusion suppress equilibrium phase transformations and promote the formation of a fine

Table 3. Influence of heat-treatment temperature on microhardness and hardness anisotropy of DMLS Ti6Al4V alloy

Condition	HV5⊥	HV5∥	A_HV = HV5⊥/HV5∥	Tukey group (HV5⊥ / HV5∥)
As-built	401.7 ± 20.8	372.7 ± 13.4	1.078	a / a
650 °C / 2 h	387.7 ± 13.6	361.3 ± 7.0	1.073	ab / a
750 °C / 2 h	371.0 ± 9.6	341.6 ± 10.5	1.086	b / b
850 °C / 2 h	351.0 ± 7.6	337.6 ± 10.0	1.040	c / b
950 °C / 2 h	326.0 ± 5.6	321.3 ± 4.7	1.015	d / c

Note: Values are presented as mean ± standard deviation. A_HV = HV5⊥/HV5∥. Different letters indicate statistically significant differences between heat-treatment conditions within the same measurement plane according to Tukey HSD ($p < 0.05$).

acicular martensitic structure, which contributes to increased resistance against plastic deformation.

A progressive decrease in hardness was observed with increasing annealing temperature. Following heat treatment at 650 °C, only a modest reduction in hardness was detected, suggesting that stress relaxation was the dominant metallurgical process occurring at this temperature. The hardness values remained relatively close to those measured in the as-built condition, indicating that the α′ martensitic structure was largely preserved.

More pronounced changes occurred after annealing at 750 °C and 850 °C. At these temperatures, hardness decreased by approximately 8% and 13%, respectively, relative to the as-built condition. The reduction is attributed to the onset and subsequent progression of α′ morphological changes consistent with martensite decomposition into the lamellar α + β-type microstructure. The increasing fraction of the softer β phase reduces resistance to indentation and promotes a more homogeneous microstructural response.

The lowest hardness values were obtained after heat treatment at 950 °C. Under this condition, hardness decreased to 326.0 ± 5.6 HV5 on the perpendicular plane and 321.3 ± 4.7 HV5 on the parallel plane. Compared with the as-built state, these values represent reductions of approximately 19% and 14%, respectively. Such behaviour is consistent with extensive morphological changes consistent with martensite decomposition, coarsening of the lamellar structure, and substantial reduction of residual stresses accumulated during layer-by-layer fabrication.

Besides the overall decrease in hardness, heat treatment also significantly affected material anisotropy. In the as-built condition, the difference between perpendicular and parallel measurements reached approximately 29 HV5. This difference decreased overall with increasing annealing temperature and was reduced to less than 5 HV5 after heat treatment at 950 °C. The trend was not strictly monotonic, as a slightly higher anisotropy coefficient was recorded at 750 °C (Table 3); this local fluctuation reflects a faster initial decrease of the parallel-plane hardness relative to the perpendicular plane and lies within the measured scatter.

To quantify this effect, an anisotropy coefficient was calculated as the ratio between hardness measured on perpendicular and parallel planes:

$$A_{HV} = HV\perp / HV\parallel \quad (3)$$

The anisotropy coefficient decreased from 1.078 in the as-built condition to 1.015 after annealing at 950 °C, indicating an almost complete disappearance of directional hardness dependence. One-way ANOVA showed a significant effect of heat-treatment condition on both HV5⊥ and HV5∥ values (HV5⊥: $F(4,40) = 50.48$, $p < 0.001$; HV5∥: $F(4,40) = 40.10$, $p < 0.001$). Tukey's post hoc test confirmed that the most pronounced differences occurred between the as-built/650 °C conditions and the 850–950 °C conditions.

The gradual reduction in hardness anisotropy can be explained by partial elimination of directional martensitic colonies and relaxation of residual stresses generated during rapid solidification. The thermally induced transformation toward a more stable α + β-type microstructure reduces the influence of build direction on local deformation mechanisms and promotes a more isotropic mechanical response.

Overall, the obtained results demonstrate that post-processing heat treatment significantly alters the hardness behaviour of DMLS Ti6Al4V alloy. While the as-built material exhibits high hardness and pronounced anisotropy, increasing annealing temperature progressively softens the alloy and reduces directional differences, particularly above 850 °C. These changes are expected to strongly

influence fracture resistance and energy absorption capability during dynamic loading, which are discussed in the following section.

Effect of heat treatment on Charpy impact toughness

The results of Charpy impact testing performed on DMLS-produced Ti6Al4V alloy subjected to various heat-treatment conditions are presented in Table 4. A substantial increase in impact toughness was observed with increasing annealing temperature, indicating a progressive improvement in the material's ability to absorb fracture energy under dynamic loading conditions.

The lowest mean impact toughness was recorded for the as-built specimens, which absorbed 14.29 ± 2.50 J/cm² before fracture. This relatively low toughness is characteristic of the acicular martensitic morphology formed during rapid solidification in the DMLS process. In addition to the limited plasticity of the martensitic morphology, residual stresses and process-induced defects contribute to localised stress concentration and premature crack initiation during impact loading.

One-way ANOVA indicated a significant effect of heat-treatment temperature on mean Charpy impact toughness ($F(4,10) = 21.09$, $p < 0.001$). Tukey's post hoc analysis indicated that the as-built and 650 °C conditions formed the lowest toughness subset, whereas the 850 °C and 950 °C conditions formed the highest toughness subset. The difference between 850 °C and 950 °C was not statistically significant, which should be interpreted in the context of the limited number of Charpy specimens and the observed standard deviations.

A slight increase in impact toughness was observed after annealing at 650 °C, where Kc reached 18.32 ± 4.10 J/cm². Although the increase was modest, the result indicates the beneficial effect of residual stress relaxation. At this temperature, microstructural changes remain limited and the α′ martensitic morphology is largely preserved; consequently, only a moderate improvement in impact resistance is achieved.

More pronounced changes occurred after heat treatment at 750 °C. The impact toughness increased to 31.56 ± 7.00 J/cm², corresponding to an improvement of more than 120% relative to the as-built condition. This increase coincides with the onset of morphological changes consistent with martensite decomposition and the formation of a mixed α + β-type microstructure, which facilitates local plastic deformation and delays unstable crack propagation.

A further increase in toughness was observed after annealing at 850 °C, where Kc reached 45.66 ± 7.20 J/cm². At this stage, the impact toughness was more than three times higher than in the as-built condition. The enhanced fracture resistance can be attributed to the development of a more homogeneous lamellar α + β structure and the increasing participation of the ductile β phase in energy dissipation mechanisms.

The highest impact toughness was obtained after heat treatment at 950 °C, reaching 52.41 ± 8.50 J/cm². Compared with the as-built state, this represents an increase of approximately 267%. The observed improvement confirms that extensive decomposition of α′ martensite and significant reduction of residual stresses substantially enhance the material's resistance to dynamic fracture.

The evolution of impact toughness demonstrates that heat treatment has a considerably stronger influence on fracture resistance than on hardness reduction. While hardness decreased by approximately 19% on the perpendicular plane over the investigated temperature range, impact toughness increased by nearly four times. This behaviour indicates that the thermally induced microstructural transformations primarily improve the material's ability to dissipate fracture energy rather than merely reducing resistance to plastic deformation.

An additional consequence of heat treatment was the reduction of orientation-dependent

Table 4. Influence of heat-treatment temperature on Charpy impact toughness and impact-toughness anisotropy of DMLS Ti6Al4V alloy

Condition	K_c⊥ (XZ) [J/cm²]	K_c∥ (XY) [J/cm²]	Mean K_c [J/cm²]	A_Kc = K_c⊥/K_c∥	Difference [%]
As-built	16.65 ± 4.96	11.92 ± 3.32	14.29 ± 2.50	1.397	39.7
650 °C / 2 h	21.30 ± 5.20	17.45 ± 4.80	18.32 ± 4.10	1.221	22.1
750 °C / 2 h	33.10 ± 7.50	30.00 ± 6.60	31.56 ± 7.00	1.103	10.3
850 °C / 2 h	46.24 ± 8.67	45.09 ± 9.91	45.66 ± 7.20	1.026	2.6
950 °C / 2 h	53.20 ± 8.90	51.60 ± 8.30	52.41 ± 8.50	1.031	3.1

mechanical behaviour. In the as-built condition, impact toughness exhibited clear anisotropy associated with the directional microstructure generated during layer-by-layer fabrication. Measurements performed in the present study on vertically and horizontally fabricated specimens revealed toughness values of 16.65 ± 4.96 J/cm² and 11.92 ± 3.32 J/cm², respectively, corresponding to a difference of approximately 40%.

Following heat treatment at 850 °C, the difference between the two orientations became negligible. Impact toughness values of 46.24 ± 8.67 J/cm² for the XZ specimens and 45.09 ± 9.91 J/cm² for the XY specimens indicate nearly identical fracture resistance irrespective of build direction. The impact-toughness anisotropy coefficient, calculated as A_Kc = K_c⊥/K_c∥, decreased from 1.397 in the as-built condition to 1.026–1.031 after annealing at 850–950 °C. This observation suggests that annealing effectively suppresses the anisotropic response inherited from the additive manufacturing process. The marginally higher coefficient obtained at 950 °C (1.031) compared with 850 °C (1.026) is well within the experimental scatter of the Charpy measurements and is therefore not considered physically significant; both conditions can be regarded as effectively isotropic.

The substantial increase in impact toughness observed after heat treatment highlights the importance of post-processing for engineering applications requiring high fracture resistance. Although the as-built condition provides elevated hardness, the associated martensitic microstructure exhibits limited energy absorption capability. In contrast, annealed specimens demonstrate significantly improved damage tolerance while maintaining mechanical properties suitable for structural and biomedical applications.

The observed toughness evolution is closely linked to the corresponding changes in hardness. As heat treatment temperature increases, the gradual reduction in hardness is accompanied by a substantial increase in fracture energy absorption. This inverse relationship suggests the existence of a characteristic hardness–toughness trade-off, which is analysed in the following section.

Relationship between microhardness and impact toughness

To better understand the mechanical response of heat-treated DMLS Ti6Al4V alloy, the relationship between microhardness and impact toughness was analysed (Figure 3). The results revealed a clear inverse correlation between both properties, indicating that thermal exposure progressively shifts the material from a hard and relatively brittle condition toward a softer but significantly tougher state.

The as-built specimens exhibited the highest hardness and the lowest impact toughness among all investigated conditions. This behaviour is characteristic of the fine acicular α′ martensitic microstructure generated during rapid cooling in the DMLS process. Although α′ martensite provides excellent resistance to plastic deformation, it offers limited capability for stress redistribution ahead of a propagating crack. Consequently, a fracture occurs with relatively low energy absorption and limited plastic deformation.

Heat treatment progressively altered this behaviour. At 650 °C, a slight reduction in hardness was accompanied by a modest increase in impact toughness, suggesting that residual stress relaxation represented the dominant mechanism influencing mechanical performance. The microstructure remained largely martensitic, and therefore, the overall fracture response changed only moderately.

A more substantial shift occurred between 750 °C and 850 °C. Within this temperature range, hardness decreased considerably while impact toughness increased rapidly. This behaviour corresponds to the active decomposition of α′ martensite and the formation of an equilibrium α + β-type microstructure. The presence of β phase regions promotes local plastic deformation and facilitates stress redistribution around microstructural discontinuities, thereby increasing the energy required for crack propagation.

The most pronounced mechanical transformation was observed after annealing at 950 °C. At this temperature, the alloy exhibited the lowest hardness and the highest impact toughness measured in the present study. The nearly complete decomposition of α′ martensite, together with significant stress relaxation and microstructural homogenisation, resulted in a material capable of absorbing substantially greater amounts of impact energy prior to fracture.

The obtained results illustrate the classical strength–toughness trade-off commonly observed in titanium alloys. High hardness is generally associated with increased resistance to localised plastic deformation but often leads to reduced fracture resistance. Conversely, microstructural softening promotes greater ductility and energy

dissipation during crack propagation. In the present study, this trade-off was particularly evident because the reduction in hardness was relatively moderate compared with the magnitude of the toughness improvement.

From an engineering perspective, the results indicate that hardness alone is insufficient for assessing the structural performance of additively manufactured Ti6Al4V components. While the as-built condition provides maximum hardness, it simultaneously exhibits the lowest resistance to dynamic fracture. Therefore, optimisation of post-processing parameters should focus not solely on preserving hardness but also on achieving an appropriate balance between strength, toughness, and microstructural stability.

The relationship between hardness and toughness additionally explains the progressive changes observed in fracture morphology. High-hardness specimens fractured predominantly through quasi-brittle mechanisms characterised by cleavage-like facets and defect-sensitive crack initiation. As hardness decreased following annealing, fracture surfaces became increasingly dominated by microvoid coalescence and ductile tearing. Consequently, the hardness–toughness relationship can be directly linked to the transition of fracture mechanisms observed during SEM analysis.

These findings demonstrate that post-processing heat treatment acts as an effective tool for tailoring the mechanical performance of DMLS Ti6Al4V alloy. By controlling the extent of morphological changes consistent with martensite decomposition and microstructural homogenisation, it is possible to regulate the balance between hardness and fracture resistance according to specific application requirements. The corresponding evolution of fracture morphology is discussed in detail in the following section.

Fractographic analysis and fracture mechanism transition

Scanning electron microscopy revealed substantial differences in fracture surface morphology between the as-built and heat-treated specimens. The observed changes corresponded closely with the evolution of microhardness and impact toughness described in the previous sections, confirming that post-processing heat treatment fundamentally altered the fracture mechanisms operating in DMLS-produced Ti6Al4V alloy.

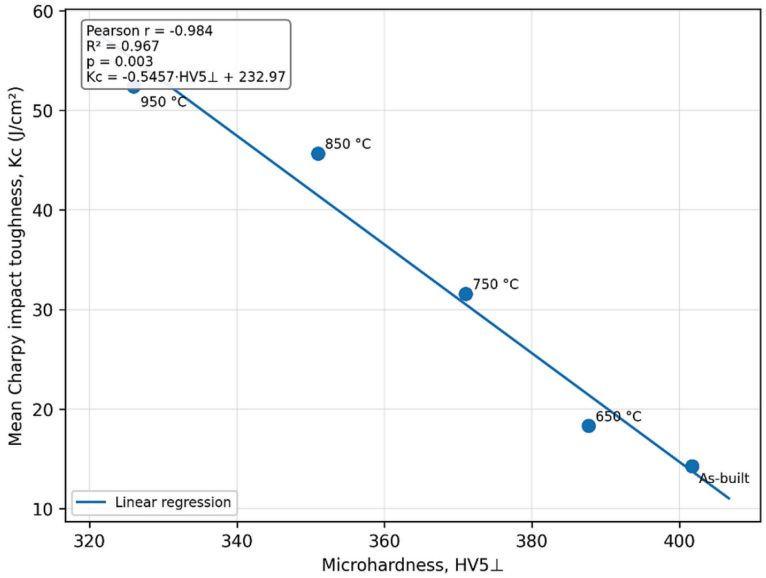


Figure 3. Relationship between microhardness and Charpy impact toughness of DMLS Ti6Al4V after post-processing heat treatment. Scatter plot showing the relationship between microhardness measured on the plane perpendicular to the deposited layers (HV5⊥) and mean Charpy impact toughness (Kc) for the as-built condition and for specimens annealed at 650, 750, 850, and 950 °C. A strong inverse correlation was observed between both properties, indicating that the progressive decrease in hardness was accompanied by a marked increase in impact toughness. Linear regression analysis yielded a Pearson correlation coefficient of r = -0.984, with R^2 = 0.967 (p = 0.003), confirming a strong hardness–toughness trade-off. he regression uses five condition-level mean pairs; microhardness values derive from at least nine indentations per plane, and Charpy means from n = 3 specimens per orientation and condition.

Representative fracture surfaces obtained for all investigated conditions are presented in Figure 4. Based on the fractographic observations, three characteristic fracture regimes were identified:

- quasi-brittle fracture (as-built and 650 °C),
- mixed-mode fracture (750 °C),
- predominantly ductile fracture (850 °C and 950 °C).

The fracture surface of the as-built specimens (Figure 4a) exhibited a heterogeneous morphology consisting of microvoid coalescence combined with localised quasi-cleavage regions. Numerous process-induced pores and irregular discontinuities were observed throughout the fracture surface and frequently acted as preferential crack initiation sites. The relatively limited density of dimples suggests restricted plastic deformation prior to fracture, which is consistent with the low impact toughness measured in the as-built condition.

After annealing at 650 °C (Figure 4b), the fracture morphology remained generally similar to that observed in the as-built material. However, a greater density of dimples and ductile tearing features became apparent. Although pores and local flat fracture regions were still present, their influence on crack propagation appeared less pronounced. These observations suggest that heat treatment at 650 °C promoted partial stress relaxation while producing only limited changes in the overall fracture behaviour.

More noticeable modifications were observed after heat treatment at 750 °C (Figure 4c). Fracture surfaces displayed an increased contribution of microvoid coalescence accompanied by a more uniform distribution of dimples. The relative fraction of flat fracture regions decreased, indicating enhanced plastic deformation prior to failure. This morphological evolution coincided with the significant increase in impact toughness observed for this condition.

The specimens annealed at 850 °C (Figure 4d) exhibited predominantly ductile fracture characteristics. The fracture surfaces were characterised by densely distributed dimples and well-developed ductile tearing ridges, indicating extensive local plastic deformation. The influence of process-related defects on crack propagation appeared reduced compared with the lower-temperature conditions, suggesting improved resistance to defect-assisted fracture.

The most developed ductile morphology was observed after annealing at 950 °C (Figure 4e). Fracture surfaces contained abundant fine dimples and extensive microvoid coalescence distributed across large areas of the fracture surface. Although isolated pores remained visible, the fracture process was dominated by plastic deformation mechanisms. The high density and uniform distribution of dimples correlate well with the highest impact toughness values recorded in the present study.

Overall, the fractographic observations demonstrate that post-processing heat treatment progressively increases the contribution of ductile deformation mechanisms during fracture. Rather than producing an abrupt transition between distinct fracture modes, annealing promotes a gradual enhancement of plastic energy dissipation through microvoid nucleation, growth and coalescence. The increasing density of dimples and the reduced influence of process-related defects provide direct microstructural evidence explaining the substantial improvement in impact toughness observed after heat treatment.

The observed evolution of fracture mechanisms closely followed the changes in mechanical performance induced by heat treatment. High-hardness specimens exhibited quasi-brittle fracture characterised by cleavage-like features and defect-sensitive crack initiation. As annealing temperature increased, the reduction in hardness was accompanied by progressively greater participation of ductile fracture mechanisms.

The transition from brittle-like to ductile fracture occurred simultaneously with the increase in impact toughness and the reduction of anisotropy. This relationship confirms that heat treatment modifies not only the numerical values of mechanical properties but also the fundamental mechanisms governing crack initiation and propagation.

The fractographic observations provide direct microstructural evidence that post-processing heat treatment promotes a gradual transition from defect-sensitive brittle fracture toward stable ductile crack propagation. This transformation represents the principal mechanism responsible for the substantial increase in impact toughness observed after annealing.

DISCUSSION

The present study demonstrated that post-processing heat treatment exerts a profound influence on the mechanical behaviour of DMLS-produced

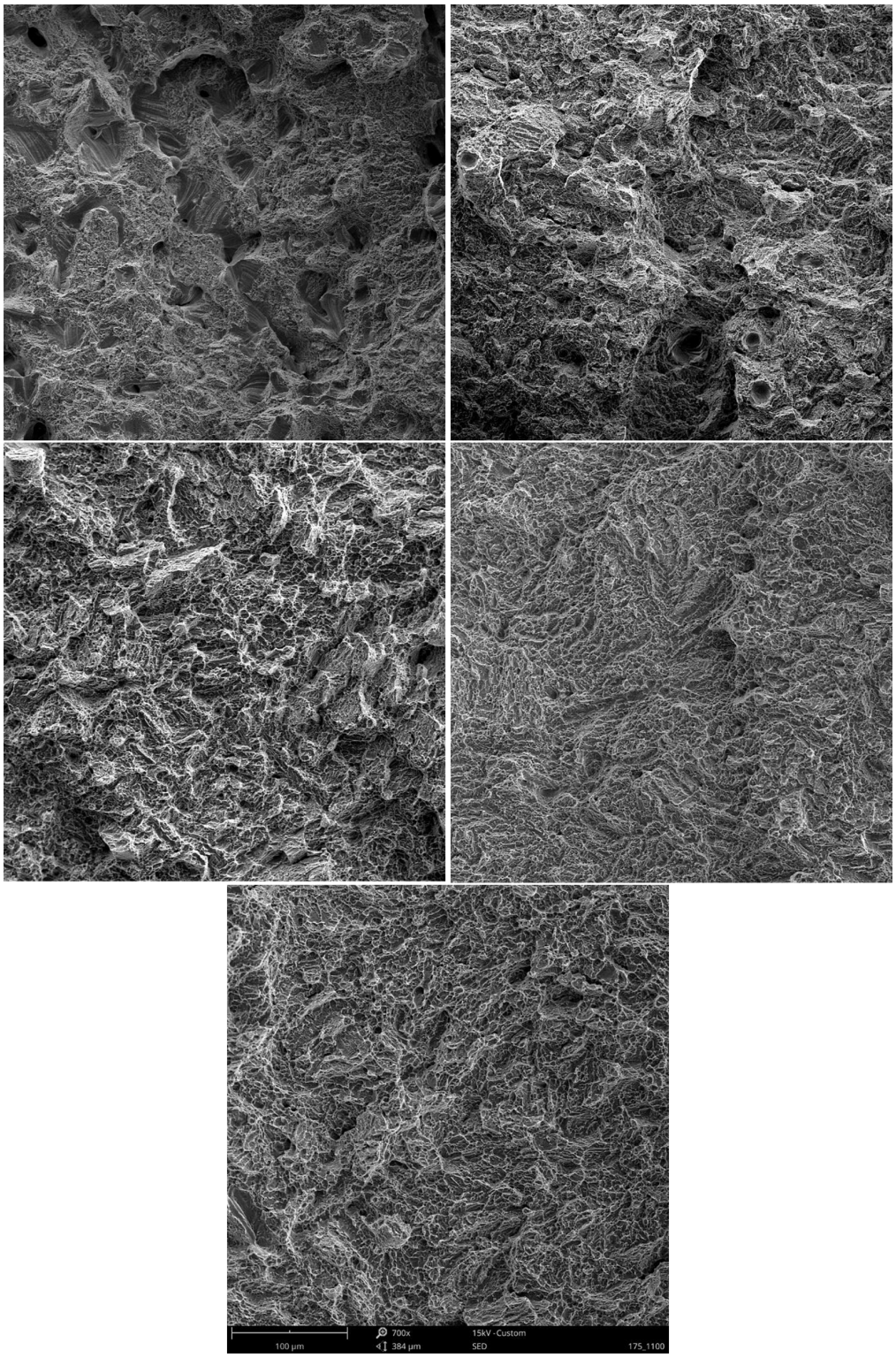


Figure 4. SEM fractographs of Charpy-tested DMLS Ti6Al4V illustrating the transition from quasi-brittle to ductile fracture with increasing annealing temperature: (a) as-built – heterogeneous surface combining limited microvoid coalescence with quasi-cleavage regions, with process-induced pores acting as crack-initiation sites; (b) 650 °C/2 h – broadly similar morphology with a higher density of shallow dimples and ductile tearing, indicating partial stress relaxation; (c) 750 °C/2 h – mixed-mode fracture with increased microvoid coalescence and a reduced fraction of flat (cleavage-like) regions; (d) 850 °C/2 h – predominantly ductile fracture characterised by densely distributed dimples and well-developed tearing ridges, with diminished influence of defects on crack propagation; (e) 950 °C/2 h – fully developed ductile morphology dominated by abundant fine dimples and extensive microvoid coalescence across the fracture surface. SEM, secondary-electron mode, 15 kV (scale bars and original magnification as indicated on each fractograph)

Ti6Al4V alloy [4,7]. The observed evolution of hardness, impact toughness, anisotropy, and fracture morphology indicates that thermal exposure fundamentally alters the microstructural state inherited from the additive manufacturing process [13]. The results reveal a progressive transition from a hard, anisotropic and relatively brittle acicular morphology toward a more homogeneous and damage-tolerant lamellar α + β-type morphology, consistent with trends reported for heat-treated LPBF Ti6Al4V [19,21].

Microstructural origin of hardness reduction

The high hardness observed in the as-built condition is characteristic of Ti6Al4V processed by laser powder bed fusion technologies. Rapid cooling suppresses equilibrium phase transformations and promotes acicular α′ martensitic morphology within elongated prior-β grains [7,8,20]. This metastable microstructure contains a high density of interfaces and lattice defects that hinder dislocation motion, resulting in elevated hardness values [4,9].

The progressive reduction in hardness observed after heat treatment is primarily associated with morphological features consistent with decomposition of α′ martensite toward a lamellar α + β-type morphology. At lower annealing temperatures, particularly at 650 °C, hardness decreases only slightly because the acicular morphology remains largely preserved and stress relaxation appears to be dominant. However, as annealing temperature increases to 750 °C and above, the acicular morphology becomes less distinct. The development and coarsening of lamellar features reduce resistance to plastic deformation and consequently lower hardness [7,13,19–21].

The largest hardness reduction was observed after annealing at 950 °C, where the alloy exhibited a decrease of approximately 19% relative to the as-built condition. Similar behaviour has been widely reported for additively manufactured Ti6Al4V and is generally considered a direct consequence of morphological changes consistent with martensite decomposition and microstructural stabilisation. The present results confirm that hardness evolution in DMLS Ti6Al4V is governed primarily by thermally induced phase transformations rather than by changes in porosity or material density. The absence of XRD or EBSD prevents direct phase confirmation; therefore, the phase interpretation should be understood as morphology-based and literature-supported, rather than crystallographically verified.

Mechanisms responsible for toughness improvement

In contrast to hardness, impact toughness increased continuously with increasing annealing temperature. The nearly fourfold increase in absorbed fracture energy observed between the as-built and 950 °C conditions represents the most significant mechanical effect identified in this study.

The relatively poor impact resistance of the as-built material can be attributed to three interacting factors. First, the fine acicular α′ martensitic microstructure formed during the rapid solidification characteristic of DMLS provides limited capability for plastic deformation ahead of the crack tip and promotes a comparatively brittle fracture response [1,7,13,14,23]. Second, high thermal gradients and repeated rapid heating and cooling cycles generate residual stresses, which increase local stress concentration and may facilitate crack initiation under dynamic loading conditions [2–4,13,14]. Third, process-induced defects, particularly gas pores, keyhole-type porosity and lack-of-fusion regions, act as preferential sites for crack initiation and reduce the effective load-bearing cross-section of the material [3,4,17,24,25].

Heat treatment progressively mitigates the microstructural and residual-stress-related contributions to poor fracture resistance. Stress relaxation decreases local stress concentration, whereas decomposition of the metastable α′ martensite promotes the formation of a more stable α + β-type microstructure with an increased capacity for plastic deformation [7,9,13,14,19,23]. Conventional annealing, however, should not be expected to eliminate pre-existing pores or lack-of-fusion defects, although the reduced residual stress level and increased ductility of the surrounding matrix may decrease their detrimental effect on crack propagation [14,17,24,25]. At higher annealing temperatures, the development and coarsening of lamellar α + β colonies provide more effective mechanisms for crack-tip blunting, crack-path deflection, and plastic energy dissipation [7,13,19,22,26]. As a result, substantially greater amounts of energy are required to initiate and propagate a crack through the heat-treated material.

The pronounced increase in impact toughness observed above 750 °C suggests that the

thermally induced transition from a fine acicular martensitic morphology toward a lamellar α + β-type morphology constitutes the dominant mechanism controlling fracture resistance [7,9,13,14,19,23,26]. The increasing capacity for local plastic deformation appears particularly important because it facilitates crack-tip blunting, redistributes stresses ahead of the crack, and delays the onset of unstable crack growth [7,12,14,26]. Consequently, the fracture process becomes progressively controlled by energy-consuming deformation mechanisms rather than by rapid brittle crack propagation. Similar heat-treatment-induced improvements in ductility, fracture resistance, and Charpy impact response have been reported for LPBF-produced Ti6Al4V and Ti6Al4V-ELI after sub-transus annealing and multi-stage heat treatment [7,12–14,26].

Reduction of manufacturing-induced anisotropy

One of the most important findings of the present investigation is the progressive reduction of anisotropic mechanical behaviour following heat treatment. In the as-built condition, both hardness and impact toughness exhibited clear directional dependence associated with the layer-by-layer manufacturing strategy and the strongly directional thermal history characteristic of DMLS processing [1,4,6,17].

The anisotropic response originates from several microstructural features inherent to laser powder bed fusion. Elongated prior β grains grow preferentially along the build direction as a result of epitaxial solidification and steep thermal gradients, while repeated thermal cycling produces directionally arranged acicular α′ martensite and heterogeneous residual-stress distributions [3,4,6,13,14,18]. The orientation of prior β grains, martensitic laths, and melt-pool boundaries relative to the loading direction can therefore influence local deformation, crack initiation, and crack propagation mechanisms [4,6,14,21]. Process-induced defects may also exhibit orientation-dependent morphology and distribution, further contributing to differences between specimens loaded parallel and perpendicular to the build direction [3,6,17,24].

The reduction in anisotropy observed after annealing indicates that heat treatment promotes microstructural and mechanical homogenisation. Decomposition of the metastable α′ martensite, redistribution of alloying elements, and formation of a more stable α + β-type microstructure reduce differences in local deformation behaviour between individual build orientations [7–9,13,14,19,20,23]. At the same time, relaxation of residual stresses decreases the directional stress fields generated during rapid solidification and repeated thermal cycling [4,8,13,14]. These changes reduce the influence of build direction on hardness, plastic deformation, and dynamic fracture behaviour.

This effect is particularly evident after annealing at 850 °C and 950 °C, where hardness values measured on the perpendicular and parallel planes become nearly identical, and the impact-toughness differences between the XY and XZ specimens are effectively eliminated. The convergence of mechanical properties at these temperatures suggests that martensite decomposition and the development of a coarser lamellar α + β-type microstructure exert a stronger influence on the mechanical response than the original directional arrangement inherited from the DMLS process [7,9,13,14,19,22,23,26]. Nevertheless, heat treatment does not necessarily completely eliminate crystallographic texture or the elongated morphology of prior β grains; rather, it reduces their mechanical significance by homogenising the phase constitution, relieving residual stresses, and increasing the capacity for plastic deformation [6,8,13,14,19].

From an engineering perspective, reducing anisotropy is highly beneficial because it increases the predictability and reliability of component performance under multiaxial and complex loading conditions [4,6,14]. For structural and biomedical applications, a more orientation-independent mechanical response is generally preferred because it reduces build-orientation-related failure risks, facilitates the definition of design allowables, and simplifies component qualification procedures [5,6,12,14]. The results, therefore, demonstrate that appropriately selected annealing conditions can improve not only the absolute mechanical properties of DMLS Ti6Al4V but also their consistency across different build orientations.

Strength–toughness trade-off in DMLS Ti6Al4V

The inverse relationship between hardness and impact toughness identified in this study illustrates the classical strength–toughness trade-off

observed in many metallic materials. High hardness is generally associated with increased resistance to plastic deformation but a reduced capacity for crack-tip blunting and fracture-energy absorption. Conversely, improvements in toughness and ductility are commonly accompanied by some degree of material softening [7,13,14,23,26].

The present results clearly demonstrate this relationship. As hardness decreased by approximately 19% on the perpendicular plane, impact toughness increased by almost four times. Importantly, the magnitude of the toughness improvement greatly exceeded the corresponding reduction in hardness. This finding indicates that moderate microstructural softening associated with α′-martensite decomposition and the development of an α + β-type microstructure can produce disproportionately large gains in dynamic fracture resistance [7,12–14,23,26].

This behaviour can be explained by the different sensitivities of hardness and impact toughness to microstructural evolution. Hardness is primarily governed by resistance to localised plastic deformation and therefore decreases as the fine acicular α′ martensitic structure decomposes and the α lamellae progressively coarsen [9,13,19,22,23]. Impact toughness, in contrast, depends strongly on the ability of the material to undergo plastic deformation ahead of the crack tip, redistribute local stresses, deflect the crack path and dissipate energy during crack propagation [7,12,14,26]. Consequently, even a moderate decrease in hardness may be accompanied by a much greater increase in absorbed fracture energy.

The preferred thermal condition depends on the service function. For biomedical components, particularly load-bearing implants, reduced anisotropy and improved damage tolerance are critical because complex geometry and multiaxial loading make orientation-dependent crack initiation undesirable; the 850–950 °C range is therefore attractive, provided that fatigue, corrosion and biological performance are verified for the final surface state. For structural or aerospace components, the optimum may shift toward 750–850 °C when higher hardness and strength retention are prioritised, whereas 950 °C is more suitable when impact resistance and fracture-energy absorption dominate the design criterion. Thus, the present data should be used as a property-selection map rather than as evidence for one universally optimal heat-treatment cycle.

It should be emphasised, however, that bulk heat treatment governs the through-thickness microstructure and residual-stress state but does not by itself establish the surface condition that controls fatigue crack initiation in additively manufactured Ti6Al4V. Because the as-built surfaces of DMLS parts typically retain adhered partially melted particles, elevated roughness, and near-surface tensile residuals, mechanical surface post-treatments are frequently applied as a complementary finishing stage. Shot peening, in particular, introduces a compressive residual-stress layer and work-hardens the near-surface region, improving fatigue and wear performance of DMLS-processed alloys and steels [27,28], while cavitation peening has been proposed as a related surface-severe-plastic-deformation route offering comparable benefits with reduced media contamination [29]. Comparative assessments further indicate that the effectiveness of such treatments on additively manufactured Ti6Al4V depends on the underlying microstructural and porosity state, so that surface finishing and bulk annealing should be regarded as coupled rather than independent optimisation stages [30]. In the present context, the sub-transus annealing conditions identified here define a favourable bulk microstructure onto which such surface treatments could subsequently be applied when the final surface state must satisfy demanding fatigue, corrosion or biological requirements.

The results further suggest that annealing temperatures between 850 °C and 950 °C provide the most favourable compromise between hardness retention and toughness enhancement. Within this temperature range, mechanical anisotropy is largely reduced, fracture behaviour becomes predominantly ductile, and impact toughness approaches the range reported for heat-treated and conventionally processed Ti6Al4V alloys [7,12,14,26]. This temperature interval is sufficiently high to promote extensive decomposition of the metastable α′ martensite, redistribution of alloying elements, and development of a lamellar α + β-type microstructure, while remaining below the β-transus temperature and therefore avoiding complete transformation to a coarse prior-β-grain structure [7,9,13,14,19,22,23].

The overall relationship between microstructural state, hardness, impact toughness, and fracture mode across all investigated conditions is summarised in Table 5.

The data confirm that the progressive replacement of the fine acicular α′ morphology by a coarser lamellar α + β-type structure is accompanied by a monotonic decrease in HV5⊥, an almost fourfold increase in Kc and a clear transition from quasi-brittle to predominantly ductile fracture. These results demonstrate that the mechanical response of DMLS Ti6Al4V is controlled not simply by the reduction in hardness, but by the accompanying increase in plastic deformation capacity and the activation of more energy-consuming crack-propagation mechanisms [7,12–14,23,26].

To position the present results within the existing body of work, the measured hardness and impact toughness values were compared with literature data for additively manufactured Ti6Al4V subjected to post-processing heat treatment, as summarised in Table 6. The comparison shows good qualitative agreement with previous studies. Sub-transus annealing generally promotes decomposition of the metastable α′ martensite, formation and progressive coarsening of a lamellar α + β-type microstructure, and a corresponding reduction in hardness accompanied by increased ductility and fracture-energy absorption [9,14,19,22,23,26]. Although direct Charpy impact data for LPBF/DMLS Ti6Al4V remain less widely reported than tensile properties, the observed increase in impact toughness is consistent with studies demonstrating improved toughness and impact response after sub-transus or multi-stage heat treatment [3,14]. Furthermore, the α/α′-lath-width ranges adopted for the as-built and high-temperature annealed conditions are consistent with microstructural dimensions reported for comparable DMLS/SLM processing routes and thermal histories [9,19,22]. Minor quantitative differences between studies may arise from variations in laser-processing parameters, initial porosity, build orientation, specimen geometry, heating rate, holding time and cooling conditions [3,14,17].

ENGINEERING IMPLICATIONS

The findings of this study have important implications for the optimisation of post-processing routes applied to DMLS Ti6Al4V components. While additive manufacturing enables the production of complex geometries, the resulting martensitic microstructure may not always provide the most desirable balance of mechanical properties.

The results demonstrate that post-processing heat treatment should not be viewed solely as a stress-relief operation. Instead, it represents a powerful tool for tailoring fracture behaviour, controlling anisotropy and improving damage tolerance. Depending on application requirements, heat treatment parameters can be selected to achieve specific combinations of hardness and toughness.

For biomedical implants, where resistance to sudden failure is critical, enhanced toughness may be particularly beneficial. Similarly, aerospace components exposed to dynamic loading may benefit from the increased fracture resistance and reduced anisotropy achieved through high-temperature annealing, in line with reports linking post-processing heat treatment to improved fatigue and damage-tolerance behaviour in additively manufactured Ti6Al4V [24,32]. Consequently, optimisation of heat treatment should be considered an integral stage of the manufacturing process rather than a secondary post-processing operation.

LIMITATIONS AND FUTURE WORK

Several limitations affect the accuracy, causal interpretation and reproducibility of the findings. First, the Charpy series comprised n = 3 specimens per orientation and condition; consequently, the large overall temperature effect is robust, but differences between adjacent

Table 5. Summary of microstructural evolution and mechanical response

Condition	Dominant microstructure	HV5⊥	Kc [J/cm²]	Fracture mode
As-built	Acicular martensitic morphology	401.7	14.29	Quasi-brittle
650 °C	Relaxed acicular morphology	387.7	18.32	Quasi-brittle
750 °C	Transitional acicular/lamellar morphology	371.0	31.56	Mixed-mode
850 °C	Lamellar α + β-type morphology	351.0	45.66	Ductile
950 °C	Coarse lamellar α + β-type morphology	326.0	52.41	Ductile

Table 6. Numerical comparison with literature values for additively manufactured Ti6Al4V after post-processing heat treatment

Source / condition	Process and heat treatment	Hardness [HV]	Impact toughness or fracture metric	Main comparison with present study
Present study	DMLS Ti6Al4V, as-built to 950 °C / 2 h, Ar; furnace cooling to 500 °C + air cooling	401.7 → 326.0 HV5	14.29 → 52.41 J/cm2	Four-temperature annealing series; A_HV decreased from 1.078 to 1.015 and A_Kc from 1.397 to approx. 1.03.
Mierzejewska et al., 2019	DMLS Ti6Al4V, optimized biomedical processing; heat treatment at approx. 850 °C	Hardness decreased after heat treatment; α/α′ lath width: 0.593 ± 0.261 →1.55 ± 0.223 µm	Tensile/fractographic response: UTS approx. 1158 → 924 MPa; YS approx. 1122 → 805 MPa; elongation approx. 4-5.5% → 12.6-16.0%; more ductile fracture after heat treatment	Supports the lath-width range used here for the as-built and 850 °C conditions and confirms reduction of anisotropy after heat treatment.
Tao et al., 2018 / SLM Ti6Al4V annealing literature	SLM Ti6Al4V annealed near 900 °C	Not central in cited comparison	Average α-lath width about 2 µm after annealing at 900 °C	Supports the plausibility of using approx. 2.3 µm for the 950 °C condition in the present sub-transus annealing series.
Zhang et al., 2021	LPBF Ti6Al4V; post-heat treatments below β-transus, including 800, 850 and 900 °C with air cooling	Not reported in the abstracted source	Charpy toughness increased by almost 100% compared with the as-built sample; α lamella thickness and β volume fraction increased with heat-treatment temperature	Confirms that sub-transus annealing improves toughness and increases lamellar coarsening in LPBF Ti6Al4V.
Cao et al., 2021 review	Review of LPBF Ti6Al4V process, post-processing, microstructure and properties	General structure-property trend: lamellar width affects strength; fine LPBF microstructure supports high strength	Coarser α+β/ Widmanstätten-type microstructures are generally favorable for fracture toughness and creep resistance	Provides broader literature context for the hardness-toughness trade-off observed in the present study.
Boccardo et al., 2024	AM Ti6Al4V; in-situ multistep heating from 400 °C to near β-transus	Not the primary endpoint	β nucleated mainly at α′-lath boundaries; full decomposition may occur at 650 °C with sufficient time, while visible coarsening became evident at ≥700 °C	Supports the metallurgical rationale for selecting 650 and 750 °C as stress-relief/ decomposition-onset and transition conditions.
Ferrari et al., 2024	LPBF Ti6Al4V; annealing at 800 and 835 °C with different holding times	Strength decreased moderately while ductility and property consistency improved	α′→α+β transformation and residual-stress reduction; 835 °C provided a favourable strength–plasticity balance	Supports the present identification of the 850 °C region as a practical compromise rather than merely a maximum-temperature condition.
Nguyen et al., 2024	Biomedical SLM Ti6Al4V; 850 °C/2.5 h, 950 and 1020 °C/1 h; furnace cooling	As-built ≈400/370 HV (top/side); heat-treated ≈348/343 HV	Lamellar α+β stabilization and reduced directional hardness difference	Closely agrees with the present hardness decrease and convergence of perpendicular/parallel values at 850–950 °C.
Squillaci et al., 2025	PBF-LB Ti6Al4V; hot isostatic pressing	HIP reduced defect sensitivity and modified fracture-energy anisotropy	Fracture energy remained linked to macrozones and microstructural directionality	Confirms that post-processing can improve damage tolerance, but also that retained texture/ macrozones may continue to influence fracture response.
Shuai et al., 2026	LPBF Ti6Al4V; systematic variation of laser power, scanning speed and hatch distance	Mechanical properties varied with process-specific microstructure rather than VED alone	Process parameters controlled prior-β morphology and α′ features	Provides current context that the present conclusions apply to the specified DMLS processing window and should not be generalized solely from VED.

high-temperature groups, especially 850 and 950 °C, have lower statistical precision. Second, the absence of XRD and EBSD means that α′ decomposition and α + β formation are inferred from SEM morphology and established transformation behaviour, rather than directly confirmed crystallographically. Third, porosity and lack-of-fusion defects were assessed qualitatively, so uncontrolled between-specimen defect variation may contribute to Charpy scatter. Fourth, α-lath/lamella widths were literature-calibrated SEM estimates, rather than measurements from a prospectively archived ImageJ dataset. Fifth, fractographic classification was semi-quantitative and based on representative fields rather than randomized stereological mapping. These constraints do not invalidate the strong monotonic hardness reduction, toughness increase or anisotropy convergence, but they limit the precision of absolute microstructural metrics and the reproducibility of fine between-condition comparisons. Future studies should therefore use larger Charpy cohorts, preregistered multi-field SEM image sampling, automated dimple/facet segmentation, micro-CT porosity quantification, residual-stress measurement and XRD/EBSD phase-texture analysis.

CONCLUSIONS

The present study investigated the influence of post-processing heat treatment on the microhardness, Charpy impact toughness, anisotropy, and fracture behaviour of DMLS-produced Ti6Al4V alloy.

Based on the obtained experimental results, the following conclusions can be drawn:

1. The as-built DMLS Ti6Al4V alloy exhibited high microhardness and pronounced anisotropy associated with acicular α′-type morphology and the directional microstructure generated during layer-by-layer fabrication.
2. Annealing at 950 °C reduced perpendicular-plane microhardness from 401.7 ± 20.8 to 326.0 ± 5.6 HV5, corresponding to an 18.8% decrease; parallel-plane hardness decreased from 372.7 ± 13.4 to 321.3 ± 4.7 HV5, corresponding to a 13.8% decrease.
3. Mean Charpy impact toughness increased from 14.29 ± 2.50 J/cm² in the as-built state to 52.41 ± 8.50 J/cm² at 950 °C, representing a 266.8% increase (3.67-fold).
4. The hardness anisotropy coefficient decreased from 1.078 to 1.015 (5.8% reduction), while the impact-toughness anisotropy coefficient decreased from 1.397 to 1.031 (26.2% reduction). After annealing at 850–950 °C, the remaining orientation-dependent difference in impact toughness was only 2.6–3.1%.
5. Fractographic analysis revealed a gradual transition from quasi-brittle fracture dominated by cleavage-like facets and defect-induced crack initiation toward predominantly ductile fracture characterised by extensive microvoid coalescence and ductile tearing.
6. A strong inverse relationship was identified between microhardness and impact toughness, confirming the existence of a characteristic strength–toughness trade-off in DMLS-produced Ti6Al4V alloy. Moderate reductions in hardness resulted in disproportionately large improvements in fracture resistance.
7. The observed mechanical evolution was governed primarily by thermally induced microstructural changes, including morphological features consistent with martensite decomposition, residual-stress relaxation, and microstructural homogenisation.
8. Within the investigated conditions, 850–950 °C provided the clearest combination of increased dynamic fracture resistance, near-isotropic response, and predominantly ductile fracture. The lower end of this interval may be preferred when hardness retention is important, whereas 950 °C maximised Charpy toughness.

Overall, the results directly support the revised title and study aim: post-processing heat treatment produced a quantifiable hardness–toughness trade-off, substantially reduced manufacturing-induced anisotropy, and shifted the fracture mechanism toward ductile microvoid coalescence in DMLS Ti6Al4V.

REFERENCES

1. Mierzejewska Ż.A., Hudák R., Sidun J. Mechanical properties and microstructure of DMLS Ti6Al4V alloy dedicated to biomedical applications. Materials 2019; 12(1): 176. https://doi.org/10.3390/ma12010176
2. Herzog D., Seyda V., Wycisk E., Emmelmann C. Additive manufacturing of metals. Acta Mater. 2016; 117: 371–392. https://doi.org/10.1016/j.actamat.2016.07.019

3. DebRoy T., Wei H.L., Zuback J.S., et al. Additive manufacturing of metallic components – process, structure and properties. Prog. Mater. Sci. 2018; 92: 112–224. https://doi.org/10.1016/j.pmatsci.2017.10.001
4. Cao S., Zou Y., Lim C.V.S., Wu X. Review of laser powder bed fusion (LPBF) fabricated Ti-6Al-4V: process, post-process treatment, microstructure, and property. Light Adv. Manuf. 2021; 2: 20. https://doi.org/10.37188/lam.2021.020
5. Harun W.S.W., Manam N.S., Kamariah M.S.I.N., et al. A review of powdered additive manufacturing techniques for Ti-6Al-4V biomedical applications. Powder Technol. 2018; 331: 74–97. https://doi.org/10.1016/j.powtec.2018.03.010
6. Murthy S.V.S.N., Sivakumar D., Ramesh Narayanan P. On the anisotropy in room-temperature mechanical properties of laser powder bed fusion processed Ti6Al4V-ELI alloy for aerospace applications. J. Mater. Sci. 2022; 57: 9599–9618. https://doi.org/10.1007/s10853-022-07058-2
7. Zhang K., Kan W.H., Liu Y., et al. Microstructure control by heat treatment for better ductility and toughness of Ti-6Al-4V produced by laser powder bed fusion. Aust. J. Mech. Eng. 2021; 19(5): 680–691. https://doi.org/10.1080/14484846.2021.2004654
8. Ter Haar G.M., Becker T.H. Selective laser melting produced Ti-6Al-4V: post-process heat treatments to achieve superior tensile properties. Materials 2018; 11: 146. https://doi.org/10.3390/ma11010146
9. Boccardo A.D., Zou Z., Simonelli M., et al. Martensite decomposition kinetics in additively manufactured Ti-6Al-4V alloy: in-situ characterisation and phase-field modelling. Mater. Des. 2024; 241: 112949. https://doi.org/10.1016/j.matdes.2024.112949
10. Macek W., Martins R.F., Branco R., et al. Fatigue fracture morphology of AISI H13 steel obtained by additive manufacturing. Int. J. Fract. 2022; 235: 79–98. https://doi.org/10.1007/s10704-022-00615-5
11. Squillaci L., et al. Microstructure and mechanical properties of Ti-6Al-4V alloy fabricated using powder bed fusion–laser beam additive manufacturing process: effect of hot isostatic pressing. Mater. Sci. Eng. A. 2025; 931: 148226. https://doi.org/10.1016/j.msea.2025.148226
12. Monaheng L., du Preez W.B., Polese C. Towards qualification in the aviation industry: impact toughness of Ti6Al4V(ELI) specimens produced through laser powder bed fusion followed by two-stage heat treatment. Metals 2021; 11(11): 1736. https://doi.org/10.3390/met11111736
13. Vrancken B., Thijs L., Kruth J.-P., Van Humbeeck J. Heat treatment of Ti6Al4V produced by selective laser melting: microstructure and mechanical properties. J. Alloys Compd. 2012; 541: 177–185. https://doi.org/10.1016/j.jallcom.2012.07.022
14. Etesami S.A., Fotovvati B., Asadi E. Heat treatment of Ti-6Al-4V alloy manufactured by laser-based powder-bed fusion: process, microstructures, and mechanical properties correlations. J. Alloys Compd. 2022; 895: 162618. https://doi.org/10.1016/j.jallcom.2021.162618
15. Ferrari E., Gaiani S., Gozzi M., et al. Impact of treatment time on single annealing thermal cycle performed on Ti-6Al-4V titanium alloy specimens obtained using LPBF technology. La Metallurgia Italiana. 2024; 116(4): 39–49.
16. Nguyen M.T., et al. Heat treatment for microstructure stabilizing of biomedical Ti-6Al-4V alloy fabricated by selective laser melting. MM Science Journal. 2024: 7453–7457. https://doi.org/10.17973/MMSJ.2024_10_2024060
17. Mierzejewska Ż.A. Effect of laser energy density, internal porosity and heat treatment on mechanical behavior of biomedical Ti6Al4V alloy obtained with DMLS technology. Materials 2019; 12(14): 2331. https://doi.org/10.3390/ma12142331
18. Yadroitsev I., Krakhmalev P., Yadroitsava I. Selective laser melting of Ti6Al4V alloy for biomedical applications: temperature monitoring and microstructural evolution. J. Alloys Compd. 2014; 583: 404–409. https://doi.org/10.1016/j.jallcom.2013.08.183
19. Lakroune Y., Connétable D., Hugues J., et al. Microstructural evolution during post heat treatment of the Ti-6Al-4V alloy manufactured by laser powder bed fusion. J. Mater. Res. Technol. 2023; 24: 2157–2167. https://doi.org/10.1016/j.jmrt.2023.01.135
20. Liu J., Song B., Yan C., et al. Effects of post heat treatments on microstructures and mechanical properties of selective laser melted Ti6Al4V alloy. Metals 2021; 11: 1593. https://doi.org/10.3390/met11101593
21. Tao P., Li H.X., Huang B.Y., et al. Tensile behavior of Ti-6Al-4V alloy fabricated by selective laser melting: effects of microstructures and as-built surface quality. China Foundry 2018; 15: 243–252. https://doi.org/10.1007/s41230-018-8064-8
22. Cao S., Hu Q., Huang A., et al. Static coarsening behaviour of lamellar microstructure in selective laser melted Ti–6Al–4V. J. Mater. Sci. Technol. 2019; 35(8): 1578–1586. https://doi.org/10.1016/j.jmst.2019.04.008
23. Cao S., Chu R., Zhou X., et al. Role of martensite decomposition in tensile properties of selective laser melted Ti-6Al-4V. J. Alloys Compd. 2018; 744: 357–363. https://doi.org/10.1016/j.jallcom.2018.02.111
24. Greitemeier D., Palm F., Syassen F., Melz T. Fatigue performance of additive manufactured TiAl6V4 using electron and laser beam melting. Int. J. Fatigue 2017; 94: 211–217. https://doi.org/10.1016/j.ijfatigue.2016.05.001

25. Kasperovich G., Hausmann J. Improvement of fatigue resistance and ductility of TiAl6V4 processed by selective laser melting. J. Mater. Process. Technol. 2015; 220: 202–214. https://doi.org/10.1016/j.jmatprotec.2015.01.025.
26. Sabban R., Bahl S., Chatterjee K., Suwas S. Globularization using heat treatment in additively manufactured Ti-6Al-4V for high strength and toughness. Acta Mater. 2019; 162: 239–254. https://doi.org/10.1016/j.actamat.2018.09.064
27. Walczak M., Szala M. Effect of shot peening on the surface properties, corrosion and wear performance of 17-4PH steel produced by DMLS additive manufacturing. Arch. Civ. Mech. Eng. 2021; 21: 157. https://doi.org/10.1007/s43452-021-00306-3
28. Żebrowski R., Walczak M., Klepka T., Pasierbiewicz K. Effect of the shot peening on surface properties of Ti-6Al-4V alloy produced by means of DMLS technology. Eksploat. Niezawodn. 2019; 21(1): 46–53. https://doi.org/10.17531/ein.2019.1.6
29. Świetlicki A., Szala M., Walczak M. Effects of shot peening and cavitation peening on properties of surface layer of metallic materials – a short review. Materials 2022; 15(7): 2476. https://doi.org/10.3390/ma15072476
30. Szala M., Chocyk D., Skic A., et al. Effects of shot peening and electropolishing treatment on the properties of additively and conventionally manufactured Ti6Al4V alloy: a review. Materials 2024; 17(4): 934. https://doi.org/10.3390/ma17040934
31. Shuai Y., Liu J., Zhu J., et al. Microstructural evolution and mechanical properties of LPBF Ti-6Al-4V with different process parameters. Materials. 2026; 19: 1049. https://doi.org/10.3390/ma19061049
32. Benedetti M., Torresani E., Leoni M., et al. The effect of post-sintering treatments on the fatigue and biological behavior of Ti–6Al-4V ELI parts made by selective laser melting. J. Mech. Behav. Biomed. Mater. 2017; 71: 295–306. https://doi.org/10.1016/j.jmbbm.2017.03.024